Journal of Power Sources 183 (2008) 14–19

Contents lists available at ScienceDirect

Journal of Power Sources

journal homepage: www.elsevier.com/locate/jpowsour

A phase inversion/sintering process to fabricate nickel/yttria-stabilized zirconia hollow fibers as the anode support for micro-tubular solid oxide fuel cells

Naitao Yang[a,b], Xiaoyao Tan[b,*], Zifeng Ma[a,**]

[a] Department of Chemical Engineering, Shanghai Jiao Tong University, Shanghai 200240, China
[b] School of Chemical Engineering, Shandong University of Technology, Zibo 255049, China

ARTICLE INFO

Article history:
Received 10 April 2008
Received in revised form 1 May 2008
Accepted 1 May 2008
Available online 8 May 2008

Keywords:
Micro-tubular solid oxide fuel cells
Ni/YSZ cermet anode
Hollow fiber
Phase inversion

ABSTRACT

NiO/YSZ hollow fibers were fabricated via a combined phase inversion and sintering technique, where polyethersulfone (PESf) was employed as the polymeric binder, *N*-methyl-2-pyrrolidone (NMP) as the solvent and polyvinylpyrrolidone (PVP) as the additive, respectively. After reduction with hydrogen at 750 °C for 5 h, the porous Ni/YSZ hollow fibers with an asymmetric structure comprising of a microporous layer integrated with a finger-like porous layer were obtained, which can be served as the anode support of micro-tubular solid oxide fuel cells (SOFCs). As the sintering temperature was increased from 1200 to 1400 °C, the mechanical strength and the electrical conductivity of the Ni/YSZ hollow fibers increased from 35 to 178 MPa and from 30 to 772 S cm^{-1}, respectively but the porosity decreased from 64.2% to 37.0%. The optimum sintering temperature was found to be between 1350 and 1400 °C for Ni/YSZ hollow fibers applied as the anode support for micro-tubular SOFCs.

© 2008 Elsevier B.V. All rights reserved.

1. Introduction

Solid oxide fuel cells (SOFCs) possess many distinct advantages such as the high-energy conversion efficiency, the fuel flexibility that allows a variety of fuels including; hydrogen, natural gas, methane, gasoline and other hydrocarbons to be employed, the high tolerance to fuel impurities and the environmental friendliness for power generation as well. In the last decade, considerable efforts have been focused on SOFCs all over the world, and kilowatt range SOFC plants have been successfully constructed and are being designed for demonstration [1]. However, in order to achieve commercialization of SOFC technology, the cell costs have to be reduced remarkably, which can be achieved by; using less expensive materials, increasing the output density, improving the cell performance and reliability, and more importantly by improving fabrication techniques [2].

In recent years, micro-tubular SOFCs have attracted increasing interests due to their high-volumetric power density, good mechanical properties, good thermo-cycling behavior, and quick start-up and shut-down operations [3–12]. The intention is to find a variety of applications such as auxiliary power units for the automobile industry and power sources for portable devices. The micro-tubular SOFCs can be constructed into the anode supported [8,9], the cathode supported [10,11] or the electrolyte supported configurations [12]. Amongst them, the anode-supported configuration is commonly adopted because the nickel containing cermet support can provide good mechanical strength and allows a thin electrolyte film to be deposited on it. As a result the internal electrical resistance of the obtained fuel cells can be reduced which is essential to improving the cell output performances.

The micro-anode tubes were often prepared through the plastic mass extrusion process [6]. The as-prepared anode tubes usually have a large wall thickness so as to provide enough mechanical strength for supporting the tube precursors. This will give rise to a large resistance to the gaseous fuel diffusion during cell operations. Recently, an immersion induced phase inversion technique has been developed to fabricate ceramic hollow fiber membranes with a thin wall thickness and an asymmetric structure that greatly reduces mass transfer of the fuel and the products [13–15]. More importantly this method does not require expensive equipment and operation is also simplified. Therefore, reduction in production costs of micro-tubular SOFCs can be expected.

In this study the phase-inversion/sintering technique was employed to fabricate Ni/YSZ cermet hollow fibers as the anode support for micro-tubular SOFCs. The influence of sintering temperature on the properties of the resulting Ni/YSZ hollow fibers has been investigated.

* Corresponding author. Tel.: +86 533 2786292; fax: +86 533 2786292.
** Corresponding author. Tel.: +86 21 54742894; fax: +86 21 54742894.
E-mail addresses: cestanxy@yahoo.com.cn (X. Tan), zfma@sjtu.edu.cn (Z. Ma).

0378-7753/$ – see front matter © 2008 Elsevier B.V. All rights reserved.
doi:10.1016/j.jpowsour.2008.05.006

2. Experimental

2.1. Materials

Commercially available NiO and 3 mol% yttria-stabilized zirconia (3YSZ) powders of purity 99.9% and of particle size of 0.1–0.8 μm diameter [purchased from Yixing 3-Science Ultra-Fine Powder Co. Ltd., Yixing, China] were used as the anode materials. Polyethersulfone (PESf) [(Radel A-300), Ameco Performance, USA], *N*-methyl-2-pyrrolidone (NMP) [AR Grade, >99.8%, Kermel Chem Inc., Tianjin, China] were used as the polymer binder and the solvent to prepare the spinning solution. Polyvinylpyrrolidone (PVP, K16-18) [from Acros Organics, M_w = 8000] was used as the dispersant. Deionized water and tap water were used as the internal and external coagulant, respectively.

2.2. Spinning of the NiO/YSZ hollow fibers

A starting solution was first prepared for spinning the hollow fiber precursors. A calculated quantity of PESf, with the PVP dispersant, was dissolved in the NMP solvent in a 250 cm^3 wide-neck bottle. After the polymer solution was formed, the NiO and YSZ powders, which were dried at 120 °C for 12 h in advance, were then added gradually under stirring. The stirring was carried out continuously for at least 72 h to ensure that all the powders were dispersed uniformly in the polymer solution. After the starting solution was degassed at room temperature for 30 min, it was then transferred to a stainless steel reservoir and pressurized to 0.15 MPa (absolute pressure) using nitrogen. A spinneret with the orifice diameter/inner diameter of 3.0/1.5 mm was used to obtain the hollow fiber precursors. Deionized water and tap water were used as the internal and external coagulants, respectively. The formed hollow fiber precursors were immersed in a water bath for more than 24 h to complete the solidification process.

The hollow fiber precursors were heated in a furnace at 600 °C for 2 h to remove the organic polymer binder, followed by sintering at high temperatures (1200–1400 °C) in ambient non-flowing air atmosphere for 5 h to allow the fusion and bonding to occur. After the furnace temperature was ramped down to room temperature, the resulting NiO/YSZ hollow fibers were removed for subsequent characterization and reduction. The operating conditions employed for preparing the NiO/YSZ hollow fibers are summarized in Table 1. Fig. 1 shows the spinneret, the internal structure of the spinneret and the derived NiO/YSZ hollow fibers.

Table 1
Preparation conditions of the Ni/YSZ hollow fibers

Experimental parameters	Values
Compositions of the starting solution (wt%)	
NiO	31.9
3YSZ	25.0
PESf, Radel A-300	7.1
NMP	35.5
PVP K16-18	0.5
Spinning temperature (°C)	20
Injection rate of internal coagulant ($cm^3\ s^{-1}$)	0.1
Nitrogen pressure (absolute pressure) (MPa)	0.15
Air gap (cm)	1.5
Sintering temperature (°C)	1200–1400
Sintering time (h)	5
Reducing temperature (°C)	750
Reducing time (h)	5

2.3. Reduction of the Ni/YSZ anodes

In order to obtain the Ni/YSZ anode tubes, the sintered NiO/YSZ hollow fibers were reduced using hydrogen. A quartz reduction chamber was used to contain the NiO/YSZ hollow fiber samples, which were broken into 4 cm lengths from the above sintered fibers. Helium was used as purge gas at 200 °C, and then pure hydrogen was passed through the chamber with a flow rate of 400 $cm^3\ min^{-1}$. The reduction was performed at 750 °C for 5 h. When the temperature was cooled down to 200 °C, the samples were then purged again with helium as the temperature was ramped down to room temperature. The resulting porous Ni/YSZ anode tubes were also characterized by techniques described below.

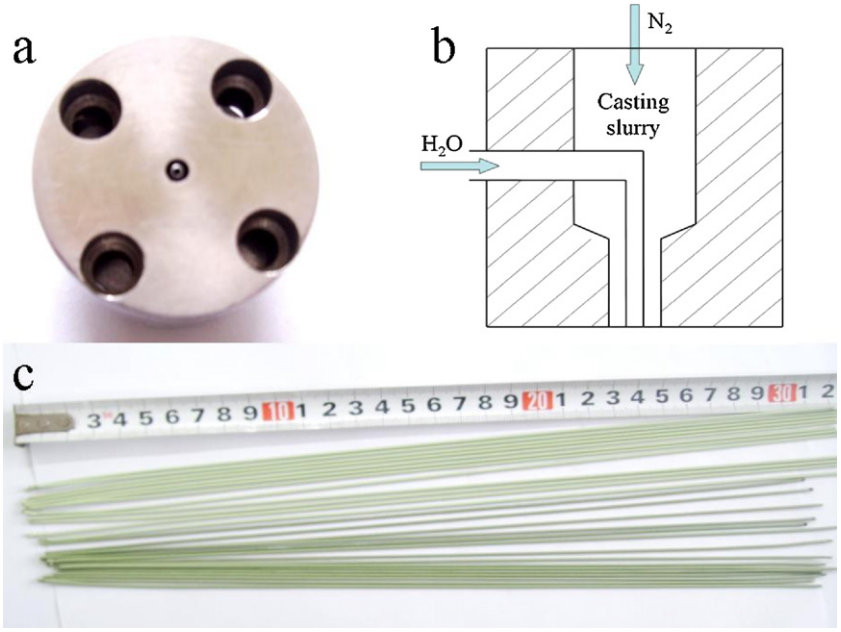

Fig. 1. Photo images of the (a) spinneret, (b) internal structure, and (c) examples of sintered NiO/YSZ hollow fibers.

2.4. Characterization methods

2.4.1. SEM

Microstructures of the NiO/YSZ and Ni/YSZ hollow fibers were ascertained by scanning electron microscopy (SEM) (FEI Sirion200, The Netherlands). Gold sputter coating was performed on the samples under vacuum before the measurements. From the SEM micrographs, the shrinkage of the anode micro-tubes at different sintering temperatures could also be calculated.

2.4.2. XRD

The crystal phases of the prepared NiO/YSZ and Ni/YSZ hollow fibers were determined by X-ray diffraction (BRUKER D8 Advance, Germany) using Cu Kα radiation ($\lambda = 0.15404$ nm). The hollow fibers were ground into fine powders prior to the XRD measurements. Continuous scan mode was used to collect 2θ data from 20° to 80° with a 0.02° sampling pitch and a 2° min^{-1} scan rate. The X-ray tube voltage and current were set at 40 kV and 30 mA, respectively.

2.4.3. Porosity

The porosity of the hollow fibers was measured using a mercury porosimeter (Quantachome Instruments PM 60-6) with a mercury pressure of 138 kPa to 275.8 MPa. Prior to measurements, the samples were heat-treated to 200 °C for 2 h. The weight of each sample taken for the measurements was around 0.8 g. In addition, the porosity of the hollow fibers was also calculated from the bulk density estimated by the weight and the corresponding dimensions of the samples.

2.4.4. Mechanical strength

The mechanical strength of the hollow fibers was measured on a three-point bending instrument (Instron Model 5544) with a crosshead speed of 0.5 mm min^{-1}. Hollow fiber samples were fixed on the sample holder at a distance of 32 mm. The bending strength, σ_F, was calculated from the following equation:

$$\sigma_F = \frac{8FLD}{\pi(D^4 - d^4)} \quad (1)$$

where F is the measured force at which fracture takes place; L, D and d are the length (32 mm), the outer diameter and the inner diameter of the hollow fibers, respectively. The values of outer diameter (D) and inner diameter (d) were obtained from the SEM graphs.

2.4.5. Conductivity

The electrical conductivity of the Ni/YSZ hollow fibers was measured at room temperature using the four-probe D.C. method on an electrochemistry workstation (Zahner IM6ex). Silver wires attached at both ends of the sample by silver paste served as the current and voltage electrodes. For reliable contact of the lead wires, Ag paste was applied to the sample and cured at 750 °C for 1 h in hydrogen atmosphere. Current–voltage characteristics were recorded in the current range of 0–1.0 A. All the samples showed nearly linear I–V curves and the electrical resistance was obtained from the slope of curves by the least square method.

3. Results and discussion

3.1. Microstructure

In this work, all the Ni/YSZ hollow fibers were obtained from the NiO/YSZ precursors spun from a dope solution with the composition of 31.9 wt% NiO, 25.0 wt% YSZ, 7.1 wt% PESf, 0.5 wt% PVP and 35.5 wt% NMP. The microstructures of the NiO/YSZ precursors at different positions are shown in Fig. 2(1a)–(1d). It can be seen that two types of porous structure, namely; the finger-like porous structure on the inner side and the sponge-like porous structure on the outer side of the hollow fibers, are present within the hollow fiber precursors. The formation of such asymmetric structure may be attributed to the different precipitation rates within the hollow fiber precursors occurring during the spinning process. The rapid precipitation occurred on the outer side due to the contact with large quantities of external coagulant resulting in the formation of microporous structure while the slow precipitation on the inner side gives rise to the macro voids or the sponge-like pores [16–18]. All the NiO and YSZ particles are well dispersed and loosely connected to each other by the polymer binder, as can be seen clearly from Fig. 2(1c) and (1d).

In order to obtain Ni/YSZ hollow fibers the NiO/YSZ precursors were sintered at high temperatures and subsequently reduced with hydrogen. The microstructures of the resultant Ni/YSZ hollow fibers sintered at 1200–1400 °C for 5 h are also shown in Fig. 2(2a)–(6d). As can be seen from (2b)–(6b), the cross-sectional structures of the Ni/YSZ hollow fibers are almost the same as that of the NiO/YSZ fiber precursor, namely, a sponge-like porous layer on the outer side integrated with a finger-like porous layer on the inner side. This suggests that the sintering only removed the organic materials but has not changed the general structure of the hollow fiber, as can be seen from (2c)–(6c). This asymmetric structure of the final Ni/YSZ hollow fibers is especially suitable for use as an anode support in SOFCs because the larger finger-like pores may provide a route with negligible resistance for transporting the fuel gas and the products while the sponge-like porous structure provides a large number of three phase boundaries (TPBs) for the electrochemical reactions. As the sintering temperature is increased from 1200 to 1400 °C, deeper sintering take place resulting in the fusion and bonding of the cermet particles as can be seen more clearly from (2c)–(6c) and (2d)–(6d). In addition, the outer surface of the hollow fibers has become more dense and smoother when sintered at higher temperature. This is of benefit in producing dense, thin electrolyte films on the outer surface for the preparation of SOFCs.

On the other hand, it also can be seen that appreciable shrinkage of the hollow fibers took place in the sintering process, not only with respect to the fiber length, but also to the wall thickness. This is a result of the removal of organic binder and the combining and sintering of the NiO and YSZ particles. Although the extent of shrinkage of the hollow fibers is a function of many factors such as the property and particle size distribution of the cermet powders, the weight ratio of cermet powder to polymer binder, the sintering conditions (such as temperature and gas environment), etc., it predictaby increases with the sintering temperature employed. Fig. 3 shows the shrinkage of the Ni/YSZ hollow fibers as a function of sintering temperature. It indicates that the hollow fibers have shrunk as much as 37.7% after being sintered at 1400 °C for 5 h. It should be mentioned that the dimensions of the hollow fibers varied little after reduction, but other properties such as the porosity and the mechanical strength have been changed due to the reduction by hydrogen, as will be discussed in the following sections.

3.2. Crystal phases

Fig. 4 shows the XRD patterns of the NiO/YSZ and the reduced Ni/YSZ hollow fibers as well as of the original YSZ powders. Note that only the XRD of the fibers sintered at 1400 °C were depicted in this figure because the others exhibit the same XRD patterns. As can be seen from the figure, no extra reflections belonging to phases other than the tetragonal phase (t-YSZ) of yttria-stabilized zirconia and the cubic nickel oxide in the NiO/YSZ hollow fiber sample

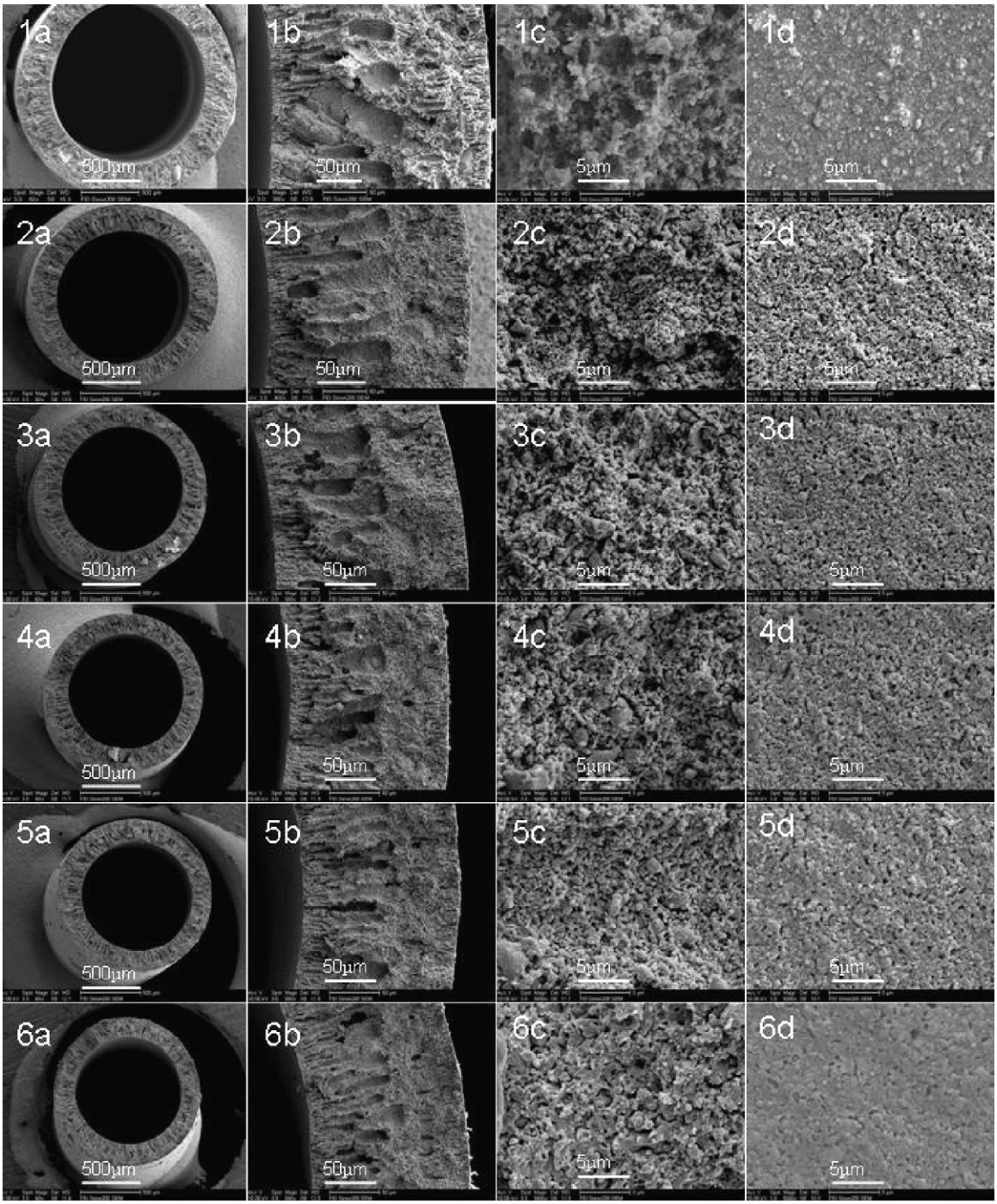

Fig. 2. SEM graphs of the NiO/YSZ precursor (1a)–(1d) and the Ni/YSZ hollow fibers sintered at 1200 °C (2a–2d); 1250 °C (3a–3d); 1300 °C (4a–4d); 1350 °C (5a–5d) and at 1400 °C (6a–6d). (1a)–(6a) for cross-sectional; (1b)–(6b) for finger-like pores; (1c)–(6c) for sponge-like pores; (1d)–(6d) for outer surface, respectively.

(Fig. 4(b)) were observed even if the sintering temperature was as high as 1400 °C. It indicates that the sample is comprised of a mixture of NiO and YSZ with no appreciable formation of new phases during the spinning and sintering process. It is known that the NiO solubility limit in the zirconia structure is ≤5 mol% for samples sintered at 1600 °C for 4 h [19], the lower sintering temperatures are believed to inhibit the solid solution formation between the two oxides [20]. However, it was also found that the intensity of the corresponding characteristic peaks of the YSZ phase in the sintered NiO/YSZ hollow fibers is much larger than those for the original YSZ powders. This suggests that the crystal size in the hollow fibers have become larger during sintering at high temperatures. After reduction all of the NiO diffraction peaks disappeared but all peaks for Ni and YSZ alone are present in the XRD pattern. It indicates that all the NiO particles have successfully transformed into Ni metal under the employed reducing conditions, i.e., 750 °C for 5 h with hydrogen flow. Since the volume of Ni is smaller than that of NiO from which it formed, the volume percent of YSZ increases after reduction leading to an increase in the YSZ peaks, as shown in the figure. It is worth noting that no detectable phase transformation or generation of new phases have appeared during the reduction process.

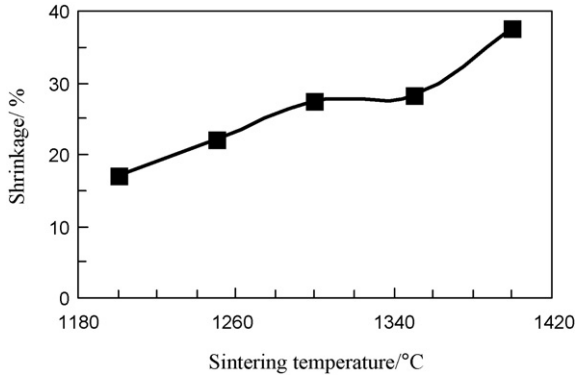

Fig. 3. Shrinkage of the Ni/YSZ hollow fibers as a function of sintering temperature.

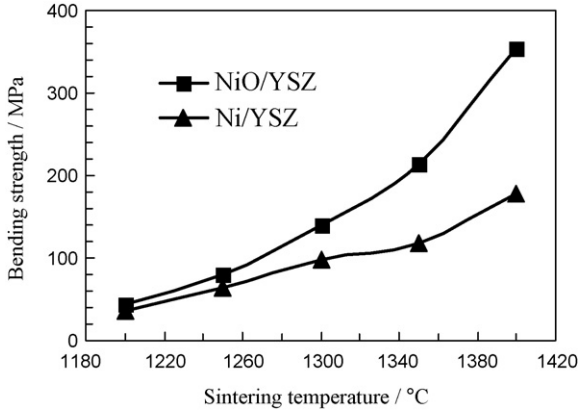

Fig. 6. Bending strength of the hollow fibers sintered at different temperatures.

3.3. Porosity

As the anode support for SOFCs, the hollow fibers should provide enough pores for transporting fuels and reaction products so that electrochemical reactions are not hindered. Fig. 5 shows the porosity of the NiO/YSZ and Ni/YSZ hollow fibers as a function of sintering temperature measured by the mercury porosimetry. As is expected, the porosity decreases with increasing the sintering temperature, which can also be corroborated from SEM. The porosity calculated from the bulk density of the hollow fibers is also plotted in the figure for comparison. It can be seen that the two porosity values are in good agreement at the lower temperatures. But for the 1400 °C sintering temperature, the calculated porosity of the hollow fibers is much higher than that measured by mercury porosimetry. Such a difference between the values may be attributed to the formation of closed pores at high-sintering temperature. According to the theory of seepage flow, the anode porosity generally should be controlled between 30% and 40% [21]. However, for the hollow fibers containing a lot of finger-like pores, this value could be higher because the larger finger-like pores provide much less TPBs for electrochemical reactions than the microporous structure. Although the porosity of the sintered Ni/YSZ hollow fibers at 1400 °C remained at 37.0%, the formation of the closed pores will deteriorate the anode performance. Accordingly, the sintering temperature should be controlled between 1350 and 1400 °C, which may give a porosity ranging from 44.5% to 37.0%.

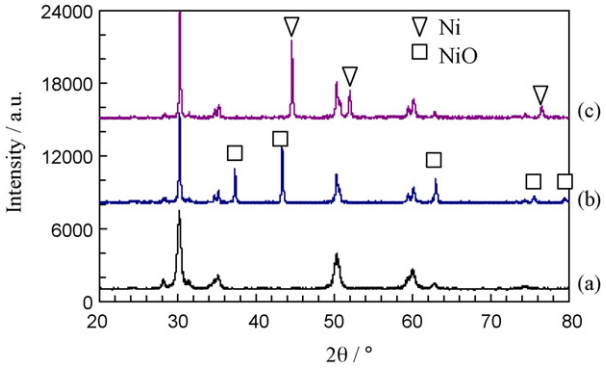

Fig. 4. XRD patterns of the (a) YSZ powder, (b) the NiO/YSZ and (c) Ni/YSZ hollow fibers sintered at 1400 °C.

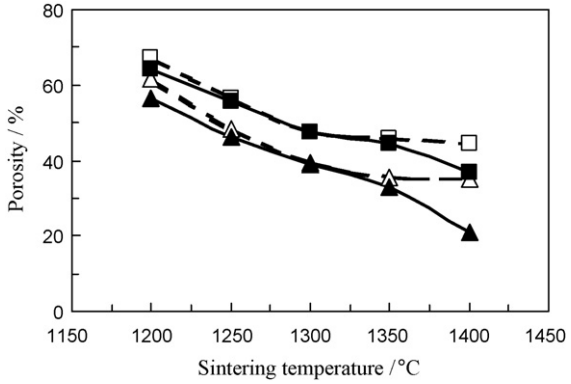

Fig. 5. Porosity of the Ni/YSZ and NiO/YSZ hollow fibers sintered at different temperatures:(▲) NiO/YSZ by mercury porosimetry; (■) Ni/YSZ by mercury porosimetry; (△) NiO/YSZ by calculation of density; (□) Ni/YSZ by calculation of density.

3.4. Mechanical strength

In order to support other components of a SOFC such as electrolyte, cathode and inter-connector, and to assemble SOFC stacks easily, the anode hollow fibers should possess sufficient mechanical strength. As described above high-temperature sintering can promote the fusion and bonding of the cermet particles. As a result, the mechanical strength of the hollow fibers is increased with increasing the sintering temperature, as shown in Fig. 6, in which the three-point bending value is plotted against sintering temperature. For the samples sintered at 1400 °C for 5 h, the three-point bending strength of the NiO/YSZ hollow fibers may reach up to 354 MPa. However, after reduction by hydrogen gas, the mechanical strength of the resulted Ni/YSZ hollow fibers would be reduced noticeably. For example, the bending strength of the sintered Ni/YSZ hollow fibers at 1400 °C is only half of that of the corresponding NiO/YSZ hollow fibers, i.e., 178 MPa. The reason for such decrease in the mechanical strength is that the loss of oxygen atoms during the reduction process not only weakens the bonding of the cermet particles but also increases of bulk porosity, as described above. Nevertheless, the reduced Ni/YSZ hollow fibers could still provide mechanical strength equivalent to that of the Ni/YSZ tubes. For example, the Ni/YSZ tubular anode fabricated by gel casting and by extrusion methods had bending strength of 112.8 and 130 MPa with the corresponding porosity of 39.6% and 28%, respectively [21,22], while the Ni/YSZ hollow fibers sintered at 1350 °C in this work have bending strength of 118.6 MPa with the corresponding porosity of 44.5%. Therefore, the phase inversion/sintering is a good method to fabricate anode micro-tubes with high strength and high porosity.

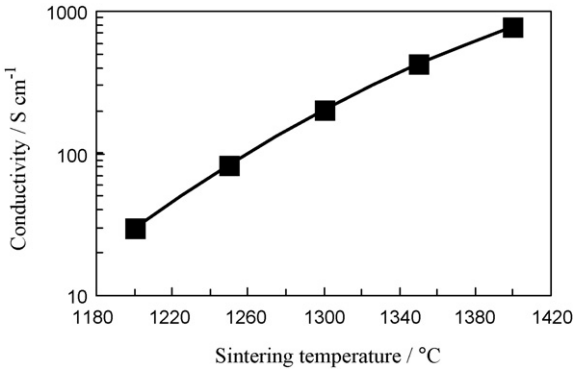

Fig. 7. Plot of conductivity of the Ni/YSZ hollow fibers against sintering temperature.

3.5. Electrical conductivity

Electrical conductivity is another important parameter for the Ni/YSZ hollow fibers in their role as the anode support of SOFCs, because it not only provides the sites for electrochemical reactions, but can also serve as a current collector. The Ni/YSZ cermet consists of two phases: one is a good electronic conductor, metallic Ni, and the other is a good ionic conductor, YSZ. In order to obtain high-electrical conductivity and high-catalytic activity, both the Ni and YSZ phases have to form continuous networks. Under this circumstance the overall conductivity of the sample is actually given by the Ni phase because the conductivity of metallic Ni is five orders of magnitude higher than that of YSZ. Fig. 7 shows the electrical conductivity of the Ni/YSZ hollow fibers sintered at different temperatures. As the sintering temperature increases, the porosity is reduced with a result of better continuity of the Ni and YSZ phases leading to the observed increase in electrical conductivity as shown in the figure. The sample sintered at 1400 °C exhibits the highest electrical conductivity, i.e., 772 S cm^{-1}, but closed pores have also been formed leading to reduced porosity of only 37.0%. Therefore, the most suitable sintering temperature lies in the range 1350–1400 °C. More detailed investigations will be carried out in our future work.

4. Conclusions

Ni/YSZ hollow fibers have been fabricated through the combined phase inversion spinning and high-temperature sintering, followed by reduction by hydrogen gas. The obtained Ni/YSZ hollow fibers possess an asymmetric structure comprising of a microporous layer integrated with a finger-like porous structure. As the sintering temperature increases, the mechanical strength and the electrical conductivity increase but the porosity of the hollow fibers decreases. The optimum sintering temperature is in the range between 1350 and 1400 °C for the Ni/YSZ hollow fibers.

Acknowledgements

The authors gratefully acknowledge financial supports from National Basic Research Program of China (973 Program, no. 2007CB209700) and Natural Science Foundation of China (no. 20676073). Dr. Alan Thursfield is acknowledged for polishing the English writing.

References

[1] M.C. Williams, J. Strakey, W. Sudoval, J. Power Sources 159 (2006) 1241–1247.
[2] W. Münch, H. Frey, M. Edel, A. Kessler, J. Power Sources 155 (2006) 77–82.
[3] T. Suzuki, Y. Funahashi, T. Yamaguchi, Y. Fujishiro, M. Awano, J. Alloys Compd. 451 (2008) 632–635.
[4] Y. Funahashi, T. Shimamori, T. Suzuki, Y. Fujishiro, M. Awano, J. Power Sources 163 (2007) 731–736.
[5] J. Pusz, A. Smirnova, A. Mohammadi, N.M. Sammes, J. Power Sources 163 (2007) 900–906.
[6] T. Suzuki, T. Yamaguchi, Y. Fujishiro, M. Awano, J. Power Sources 160 (2006) 73–77.
[7] N.M. Sammes, Y. Du, R. Bove, J. Power Sources 145 (2005) 428–434.
[8] T. Suzuki, Y. Funahashi, T. Yamaguchi, Y. Fujishiro, M. Awano, J. Power Sources 171 (2007) 92–95.
[9] T. Suzuki, T. Yamaguchi, Y. Fujishiro, M. Awano, J. Power Sources 163 (2007) 737–742.
[10] Y. Liu, S.-I. Hashimoto, H. Nishino, K. Takei, M. Mori, T. Suzuki, Y. Funahashi, J. Power Sources 174 (2007) 95–102.
[11] T. Yamaguchi, S. Shimizu, T. Suzuki, Y. Fujishiro, M. Awano, Mater. Lett. 62 (2008) 1518–1520.
[12] G.J. Saunders, K. Kendall, J. Power Sources 106 (2002) 258–263.
[13] X. Tan, S. Liu, K. Li, J. Membr. Sci. 188 (2001) 87–95.
[14] X. Tan, S. Liu, K. Li, R. Hughes, Solid State Ionics 138 (2000) 149–159.
[15] X. Tan, Z. Pang, Z. Gu, S. Liu, J. Membr. Sci. 302 (2007) 109–114.
[16] J.F. Blanco, J. Sublet, Q.T. Nguyena, P. Schaetzel, J. Membr. Sci. 283 (2006) 27–37.
[17] S. Mok, D.J. Worsfold, A.E. Fouda, T. Matsuura, S. Wang, K. Chan, J. Membr. Sci. 100 (1995) 183–192.
[18] T.-H. Young, L.-W. Chen, Desalination 103 (1995) 233–247.
[19] A. Kuzjukevics, S. Linderoth, Solid State Ionics 93 (1997) 255–261.
[20] V. Esposito, D.Z. de Florio, F.C. Fonseca, E.N.S. Muccillo, R. Muccillo, E. Traversa, J. Eur. Ceram. Soc. 25 (2005) 2637–2641.
[21] D. Dong, J. Gao, X. Liu, G. Meng, J. Power Sources 165 (2007) 217–223.
[22] Y. Du, N.M. Sammes, J. Power Sources 136 (2004) 66–71.